



저작자표시-비영리-변경금지 2.0 대한민국

이용자는 아래의 조건을 따르는 경우에 한하여 자유롭게

- 이 저작물을 복제, 배포, 전송, 전시, 공연 및 방송할 수 있습니다.

다음과 같은 조건을 따라야 합니다:



저작자표시. 귀하는 원저작자를 표시하여야 합니다.



비영리. 귀하는 이 저작물을 영리 목적으로 이용할 수 없습니다.



변경금지. 귀하는 이 저작물을 개작, 변형 또는 가공할 수 없습니다.

- 귀하는, 이 저작물의 재이용이나 배포의 경우, 이 저작물에 적용된 이용허락조건을 명확하게 나타내어야 합니다.
- 저작권자로부터 별도의 허가를 받으면 이러한 조건들은 적용되지 않습니다.

저작권법에 따른 이용자의 권리는 위의 내용에 의하여 영향을 받지 않습니다.

이것은 [이용허락규약\(Legal Code\)](#)을 이해하기 쉽게 요약한 것입니다.

[Disclaimer](#)

Inhibition of fatty acid amide  
hydrolase in the insular cortex  
produces analgesic effects in  
neuropathic rats

Min Jee Kim

Department of Medical Science

The Graduate School, Yonsei University

Inhibition of fatty acid amide  
hydrolase in the insular cortex  
produces analgesic effects in  
neuropathic rats

Min Jee Kim

Department of Medical Science

The Graduate School, Yonsei University

Inhibition of fatty acid amide  
hydrolase in the insular cortex  
produces analgesic effects in  
neuropathic rats

Directed by Professor Bae Hwan Lee

The Master's Thesis  
submitted to the Department of Medical Science  
the Graduate School of Yonsei University  
in partial fulfillment of the requirements for the degree of  
Master of Medical Science

Min Jee Kim

June 2018

This certifies that the Master's Thesis  
of Min Jee Kim is approved.

---

Thesis Supervisor : Bae Hwan Lee

---

Thesis Committee Member#1 : Jong Eun Lee

---

Thesis Committee Member#2 : Ho Sung Jung

The Graduate School  
Yonsei University

June 2018

## ACKNOWLEDGEMENTS

기대와 두려움을 안고 시작했던 학위과정, 비로소 이 길었던 모든 과정을 마무리하며 지나온 시간을 되돌아봅니다. 수많은 노력들과 시간들이 모여 논문으로 결실을 맺는 일련의 과정은 비단 학문적 배움 만이 아닌 내면의 성장이 이루어지는 시간이었습니다. 이 모든 과정이 가능하기까지 너무나 부족한 저를 지도해주신 이배환 교수님께 가장 먼저 감사의 인사를 올립니다. 교수님은 제게 연구자로서의 소양 뿐만 아니라 삶의 자세에 대한 가르침을 주셨습니다. 교수님의 제자가 되는 것은 저에게는 너무나 영광스러운 일이며, 이런 숭고한 가르침을 가슴 깊이 새기고 늘 성장할 수 있도록 하겠습니다. 또한 저에게 연세대학교 의과대학에서 학업을 시작할 수 있도록 기회를 주신 안덕선 교수님, 정승수 교수님께도 깊은 감사를 드립니다. 냉철한 시각과 혜안으로 조언을 아끼지 않으셨던 두 분 교수님 덕분에 부족한 제가 학위과정을 시작할 수 있었고 연구자의 길을 걸을 수 있었습니다. 그리고 제 논문의 심사를 맡아주시고 소중한 충고와 조언을 해주신 이종은 교수님, 정호성 교수님께 감사의 말씀 올립니다.

실험실 생활에 있어서 늘 따뜻하게 챙겨주시고 지금의 실험실이 있기까지 많은 노력과 사랑으로 지켜주신 이경희 선생님, 김은정 선생님, 사영희 선생님께도 진심으로 감사 드립니다. 선생님들의 도움이 있었기에 제가 무사히 연구를 마칠 수 있었습니다. 늘 건강하세요.

힘든 학위과정을 너무도 훌륭하게 지내오신 권민지 한정수 두 선배님께 감사인사를 드립니다. 선배님들께서 닦아 놓으신 길 덕분에 학업을 진행함에 있어 여러 방면에서 큰 도움이 되었습니다. 많이 부족한 후배였지만 선배님의 가르침이 있었기에 제 학위가 무사히 마무리 될 수 있었습니다.

학위과정 동안 가장 오랜 시간을 함께하며 매 순간 나에게 힘이 되어준 하나뿐인 소중한 동기 효진에게 감사 드립니다. 힘든 순간이 올 때마다 진

심 가득한 충고와 도움의 순간이 있었기에 긴 학위과정을 무사히 마칠 수 있었습니다. 또한 많은 시간을 함께하며 함께 울고 웃었던 선우언니, 외로울 수 있었던 학위과정 동안 큰 힘이 되어주었습니다. 감사합니다. 언니의 성실함은 나에게 긍정적인 자극이 되었고 나를 성장하게 해주었습니다. 외로울 수 있었던 학위과정 동안 큰 힘이 되어주었습니다. 후배이지만 배울 점이 많은 경민, 송연에게도 감사의 말 전합니다. 늘 성실하게 묵묵히 학업을 이어가는 모습이 나의 지난날을 돌이켜보게 하는 계기가 되었습니다. 그 누구보다 훌륭하게 학위를 진행할 두 후배들에게 부끄럽지 않은 선배가 되도록 노력하겠습니다.

포기하고 싶은 여러 순간에 늘 다독여주며 힘이 되어준 내 소중한 친구들, 지혜, 예정, 다영, 지수, 선경에게 감사의 말 전합니다. 때론 친구처럼, 가족처럼 힘든 순간에 내 옆에 있어주어 너무 든든했습니다.

사랑하는 부모님. 늦은 나이까지 학업을 이어가는 철없는 막내딸의 더딘 발걸음을 묵묵히 지켜주시고 오롯이 사랑으로 감싸주신 덕에 이 모든 것이 가능할 수 있었습니다. 부모님의 무조건적인 사랑과 저에게 주셨던 믿음에 늘 실망만 안겨드리는 것 같아 마음이 무거운 날이 많았는데 이제는 그 마음에 보답하듯 한걸음 나아갈 수 있을 것 같습니다. 지나온 모든 순간을 소중하게 간직하여 부모님에게 자랑스러운 딸이 되도록 더욱 노력하겠습니다. 사랑합니다. 가족의 따뜻함이 필요한 순간에, 선배로써 현실적인 도움이 필요할 때 늘 곁에서 힘이 되어준 언니와 형부 너무 감사합니다. 가장 친한 친구이자 학계의 선배인 언니와 형부가 내 가족이라는 것은 나에게서 커다란 행운이며 존재만으로도 힘이 되어주었습니다.

자신감을 잃고 방황하는 저에게 힘을 실어준 이모. 이모의 말씀은 저에게 정말 큰 힘이 되었으며 매 순간 발전을 꾀하는 모습으로 변화하게 하였습니다. 감사합니다.

남들보다 길었던 학위과정을 드디어 마무리하며 이제 사회로 나가 진정한

제 인생을 설계해가야 하는 시기가 도달하였습니다. 나에게는 오지 않을 것 같은 이 시간을 더욱 소중하게 생각하며 저의 학위에 도움을 주셨던 모든 분들의 노력이 헛되지 않도록 매 순간 노력하는 사람이 되도록 하겠습니다.

2018년 6월

김민지

## TABLE OF CONTENTS

ABSTRACT	1
I. INTRODUCTION	3
II. MATERIALS AND METHODS	6
1. Neuropathic pain model	6
A. Experimental animals	6
B. Cannula implantation	6
C. Neuropathic pain surgery	6
2. Behavioral test	7
A. Measuring response threshold for mechanical allodynia	7
B. URB597 microinjection into the insular cortex and analgesia test	7
3. Optical imaging	8
4. Immunohistochemistry	9
5. Western blot	10
6. Quantative real-time PCR	11
A. RNA extraction and cDNA synthesis	11

B. SYBR-Green quantitative real-time PCR	11
7. Statistical Analysis	12
III. RESULTS	13
1. Peripheral nerve injury leads to the development of mechanical allodynia	13
2. Neuropathic pain activates FAAH signaling-related factors in the IC	15
3. Expression of FAAH signaling-related proteins in the IC after nerve injury	17
4. URB597 microinjection into the IC reduces mechanical threshold	19
5. Inhibition of FAAH by URB597 reduces excitability during neuropathic pain	21
6. Inhibition of FAAH reduces neuronal activation related to IC pain	24
7. Nerve injury elevates CB1R in the insular cortex	26
8. Microinjection of URB597 into the IC increases level of NAPE-PLD	28
9. mRNA expressions of endocannabinoid components	30
IV. DISCUSSION	32

V. CONCLUSION	38
REFERENCES	39
ABSTRACT (IN KOREAN)	46
PUBLICATION LIST	48

## LIST OF FIGURES

- Figure 1. Schematic procedure of animal surgery, drug injection, behavioral test and tissue collection on POD 14 .....8
- Figure 2. Development of mechanical allodynia in neuropathic pain rats and sham-injured rats .....14
- Figure 3. mRNA expression of CB1R, NAPE-PLD and TRPV1 increases in the IC of neuropathic pain rats compared with sham operated rats .....16
- Figure 4. Changes in expression levels of FAAH-related protein in the IC of NP groups compared with sham groups .....18
- Figure 5. Microinjection of URB597 attenuates mechanical allodynia in a dose-dependent manner .....20
- Figure 6. Changes in optical signals of the IC before and after treatment with 4 nM URB597 or vehicle in nerve-injured rats .....22
- Figure 7. Changes in c-Fos expression after microinjection of URB597 in the IC .....25

Figure 8. Changes in CB1R in the IC after microinjection of 4 nM URB597 or vehicle in the NP rats.....	27
Figure 9. Effects of URB597 on the expression of CB1R, NAPE-PLD, FAAH and TRPV1 in the IC.....	29
Figure 10. Changes in mRNA levels of FAAH signaling component following URB597 microinjection into the IC.....	31
Figure 11. Schematic representation of possible synaptic mechanisms of action for AEA in neurons in the IC.....	35

## ABSTRACT

Inhibition of fatty acid amide hydrolase in the insular cortex produces analgesic effects in neuropathic rats

Min Jee Kim

*Department of Medical Science  
The Graduate School, Yonsei University*

(Directed by Professor Bae Hwan Lee)

The insular cortex (IC) is an important brain region involved in the processing of pain and emotions. Recent studies indicate that a lesion of the IC induces pain asymbolia and reverses neuropathic pain. Endogenous cannabinoids (endocannabinoids) are also known to attenuate pain; however, they are simultaneously degraded by the fatty acid amide hydrolase (FAAH), which ceases the mechanism of action. FAAH activity can be suppressed by the selective inhibitor URB597, which reduces pain by conserving endocannabinoids. The present study was conducted to examine the analgesic effects of URB597 treatment in the IC of an animal model of neuropathic pain. Under pentobarbital anesthesia, male Sprague-Dawley rats were subjected to nerve injury and assessed mechanical thresholds using the von Frey test. In the neuropathic pain group, that expression of c-Fos, CB1R, N-acyl phosphatidylethanolamine phospholipase D (NAPE-PLD), and transient receptor potential vanilloid 1 (TRPV1) increased significantly, compared with the sham-operated control group. URB597 or vehicle were administered to the IC in rats by microinjection, 14 days after nerve injury. It is found that the mechanical threshold and expression of NAPE-PLD significantly increased in groups

treated with 2 nM and 4 nM URB597 compared with the vehicle-injected group. Attenuation of neural activation was quantified by URB597 using histological analysis of c-Fos expression levels and optical imaging of the IC. These results suggest that the microinjection of FAAH inhibitor into the IC causes analgesic effects by decreasing neural excitability and increasing signaling related to the endogenous cannabinoid pathway in the IC.

---

Key words : insular cortex, neuropathic pain, FAAH (fatty acid amide hydrolase), NAPE-PLD (N-acyl phosphatidylethanolamine-specific phospholipase D), URB597

Inhibition of fatty acid amide hydrolase in the insular cortex produces  
analgesic effects in neuropathic rats

Min Jee Kim

*Department of Medical Science  
The Graduate School, Yonsei University*

(Directed by Professor Bae Hwan Lee)

## I. INTRODUCTION

Chronic pain results from conditions that compromise or incorporate nerve injury, including spinal lesion, diabetes, or other conditions.<sup>1,2</sup> Long-lasting pain interferes with an individual's social activities and impairs quality of life.<sup>3</sup> Previously, anodynes, such as anti-inflammatory drugs, anticonvulsants, and opioids, were used to treat neuropathic pain, despite their lack of efficacy or an occurrence of unexpected side effects.<sup>4</sup> Current therapeutic treatments of neuropathic pain have been frequently reported to be unsatisfactory or inefficient.<sup>1</sup> Therefore, it is necessary to search for better therapeutic targets. Neuropathic pain therapy can be improved by identifying and studying efficacious drugs and by targeting specific brain regions that are generally known to modulate pain signals.

The insular cortex (IC) is an important brain region associated with the processing of painful input and emotions.<sup>5</sup> The pain matrix, including the IC, is activated by noxious electrical and chemical stimulation and by acute and chronic pain stimulation, as

demonstrated by functional magnetic resonance imaging (fMRI).<sup>6-8</sup> Moreover, lesions of the IC diminish neuropathic pain-related behaviors in an animal model of neuropathic pain.<sup>9-12</sup>

Among the various suggested treatments for neuropathic pain, cannabinoids have become a potent analgesic target for the development of anodynia. Cannabinoids have been recognized for centuries in treatment of diverse illnesses and as having potentially useful therapeutic effects, including analgesia.<sup>13</sup> However, unfavorable side effects, such as euphoria and hyperphasia, were observed in mammals treated with plant-derived cannabinoids.<sup>14</sup> These physiological actions are produced via an endogenous cannabinoid neurotransmission system,<sup>15</sup> mainly composed of two G-protein coupled receptors, levels are abundant in the central and peripheral neurons, which mediate excitatory and inhibitory transmitters, including acetylcholine, noradrenaline, and glutamate.<sup>16,17</sup> CB1Rs were also found in pain pathways at the central terminals of primary afferent neurons in the brain and spinal cord.<sup>18</sup> These receptors are thought to mediate cannabinoid-induced analgesic effects.<sup>18</sup> Activation of CB1R in the brain inhibits the release of the excitatory neurotransmitter glutamate onto GABAergic neurons.<sup>17</sup> In contrast to CB1R expression, CB2Rs are highly expressed in the immune system and peripheral tissues.<sup>19</sup> When activated, CB2Rs can modulate cytokine release and immune cell migration.<sup>20</sup> CB2Rs are also expressed by neurons in the brain.<sup>21,22</sup> However, the role of neuronal CB2R has not yet been established.<sup>14,16</sup>

In mammalian tissues, there are two major endogenous agonists for CB1R and CB2R, respectively, N-arachidonylethanolamine (AEA, anandamide) and 2-arachidonoylglycerol (2-AG). These are synthesized 'on demand' by the postsynaptic neurons and released in retrograde across the synapse via the endocannabinoid membrane transporter to activate CB1R and CB2R that are located on the presynaptic neurons.<sup>23-26</sup> Both AEA and 2-AG are degraded rapidly by uptake of intracellular enzymes; AEA is degraded by fatty acid amide hydrolase (FAAH) and 2-AG by monoacylglycerol lipase (MAGL).<sup>27,28</sup> The binding affinity of AEA with CB1R is 24-fold less potent than 2-AG.<sup>29</sup> Additionally, synthesis of AEA forms the enzyme, N-acyl phosphatidylethanolamine phospholipase D (NAPE-PLD), which is produced in a Ca<sup>2+</sup>-dependent manner in rat brain neurons and mouse astrocytes.<sup>30</sup>

Previous research has shown that elevation of endocannabinoids causes robust

antinociception in neuropathic pain models.<sup>31,32</sup> Systemic and intrathecal administration of FAAH inhibitors has significant antinociceptive effects in preclinical models of peripheral neuropathic pain.<sup>33</sup> In particular, the selective FAAH inhibitor URB597 is reported to induce anodynia in several pain models, including heat stimulation, inflammation, and nerve injury-induced pain.<sup>34,35</sup> A previous study reported that the FAAH inhibitors significantly increased AEA levels in the brain and mainly induced CB1R-mediated antinociception. Therefore, protecting AEA from degradation may produce antinociception.<sup>36</sup>

## II. MATERIALS AND METHODS

### 1. Neuropathic pain model

#### A. Experimental animals

Male Sprague-Dawley rats (180-220 g, Koatec, Pyeongtaek, Korea) were used. They were housed in groups of three rats per cage with 12-h light/dark cycles with food and water provided *ad libitum*. All experimental procedures and surgeries were performed during the light cycle. Animals were habituated at least for a week before behavioral tests and surgery. All experimental protocols in this study were in compliance with the National Institutes of Health guidelines and approved by the Institutional Animal Care and Use Committee of Yonsei University Health System.

#### B. Cannula implantation

For cannula implantation, rats were fully anesthetized with pentobarbital sodium [50 mg/kg, intraperitoneal (i.p.)] and placed in a stereotaxic frame. The skull was exposed and a 28-gauge guide cannula was implanted in the IC (AP: +1.0 mm, ML:  $\pm 4.7$  mm, and DV: -5.8 mm). Coordinates according to the rat brain atlas of Paxinos & Watson<sup>37</sup> was selected. Implanted cannulae were anchored with three stainless-steel screws and dental acrylic cement. Each guide cannula was closed by a stainless-steel dummy cannula.

#### C. Neuropathic pain surgery

Neuropathic pain (NP) surgery was performed after cannula implantation. For the NP model, rats underwent ligation and transection of the sciatic nerve branches under anesthesia with sodium pentobarbital (50 mg/kg). Briefly, the left sciatic nerve was exposed between the mid-thigh level and carefully removed the surrounding connective tissues. The three major divisions of the sciatic nerve (tibial, sural, and common peroneal

nerves) were clearly separated. NP surgery was produced by a complete ligation and tight transection of the tibial and sural nerves with 4-0 silk sutures, leaving the common peroneal nerve intact. It is confirmed complete hemostasis and closed the muscle and skin with silk sutures. For the sham-operated animals, the left sciatic nerve was exposed, but nerve branches were left intact without injury. After all surgical procedures, the animals were injected with gentamycin to prevent postoperative infection.

## 2. Behavioral test

### A. Measuring response threshold for mechanical allodynia

To assess mechanical allodynia, paw withdrawal thresholds was measured before nerve injury and on postoperative days (PODs) 1, 4, 7, and 14 using an electronic von Frey filament (UGO Basile, Varese, Italy). Rats were placed in acrylic cages (8 x 10 x 20 cm) with wire mesh bases and allowed the rats to explore for 15 min for experimental familiarization. The electronic von Frey filament was perpendicularly pressed against the sensitive area of the left hind paw. The mechanical threshold was recorded upon the animal flinching from the touch of the von Frey filaments. Trials were conducted seven times.

### B. URB597 microinjection into the insular cortex and analgesia test.

Groups of seven animals were divided by their given dosages. Animals were gently restrained during microinjection. The dummy cannula was removed and inserted a stainless-steel injection cannula connected by polyethylene tubing (PE10) to a Hamilton syringe through the guide cannula. The rats received bilateral 1  $\mu$ l/min (per side) intra-IC administration of vehicle (1:1:8=Cremophor EL: dimethyl sulfoxide (DMSO): saline) or different doses of URB597. After microinjection, the injection cannulae remained in place for 1 min. The behavioral test was performed pre-microinjection and 30 min, 1, 2, 4, 8, 12, and 24 hr post-microinjection.

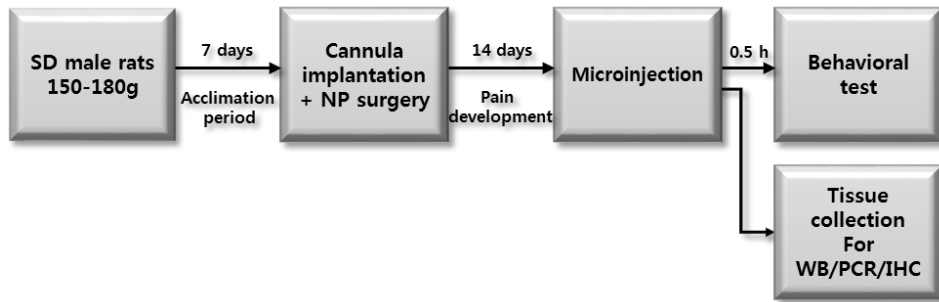


**Figure 1. Schematic procedure of animal surgery, drug injection, behavioral test and tissue collection on POD 14.**

### 3. Optical imaging

Optical imaging was performed as described in a previous article<sup>38</sup> with a slight modification. Sprague-Dawley male rats (250–300 g; n=6/group) were fully anesthetized with urethane (1.25 g/kg, i.p.) on POD14 and given atropine (5 mg/kg, i.p.) to suppress mucus secretion and dexamethasone sulfate (1 mg/kg, i.p.) to reduce swelling of the cortex. Rats were placed on their sides in a custom-made stereotaxic frame, which allowed access to the IC located in the anterolateral aspect of the brain. Endotracheal intubation was performed to minimize respiratory movements during optical imaging. Craniectomies were conducted and resected the overlying the temporalis muscle, zygomatic arch, and the dura mater to expose the cortex. The cortex was stained using a voltage-sensitive dye (di-2-ANEPEQ, 50 mg/mL in saline; Molecular Probes, Eugene, OR, USA) for 1 hr and carefully rinsed with normal saline. The optical imaging method was performed directly on the exposed cortex for 30 min before and after the application of vehicle or 4 nM URB597. Dye fluorescence was detected using a high-resolution charge-coupled device (CCD) camera (Brainvision Inc., Tokyo, Japan) equipped with a dichroic mirror with a 510–550 nm excitation filter and 590 nm absorption filter. A tungsten halogen lamp (150 W) was used for fluorescence excitation. The imaging area

was  $6.4 \times 4.8 \text{ mm}^2$  and consisted of  $184 \times 124$  pixels.

A pair of stainless-steel electrodes were implanted into the left hind paws where the electronic von Frey filament was applied during behavioral testing. The receptive field was stimulated with a square pulse (width: 0.1 ms, interstimulus interval: 5 s, intensity: 5.0 mA) using a stimulus isolation unit (World Precision Instruments, Sarasota, FL, USA). The fluorescent intensity was detected during each trial for approximately 940 ms under an optical microscope (Leica Microsystems Ltd., Heerbrugg, Switzerland) equipped with a  $1\times$  objective and a  $1\times$  projection lens. Optical signals were acquired at a rate of 3.7 ms/frame and averaged 30 times by an optical imaging recording system (MiCAM02; Brainvision Inc.). Optical imaging acquisition was triggered by electrocardiogram signals using a stimulus/non-stimulus subtraction method. Amplitudes and excitatory areas of optical signals were measured using a spatial filter ( $9 \times 9$  pixels) to reduce artifacts caused by vibration and brain movements. Using captured images, fractional changes were quantified in optical signals (optical intensity) and areas of activation. Changes in optical intensity were calculated in the IC as the percentage of fractional change in the intensity of fluorescence ( $\Delta F/F \times 100$ ). Activated areas were analyzed using the activated pixel number of an ROI / total pixel number of the ROI  $\times 100$  (previously described<sup>38</sup>). Data were analyzed with BV Analyzer software (Brainvision Inc.).

#### 4. Immunohistochemistry

Immunohistochemistry was conducted to verify the target gene of interest, using the URB597-injected brains and their vehicle controls. Under urethane anesthesia, the rats were transcardially perfused with normal saline (0.9% NaCl) followed by 4% paraformaldehyde in 0.1 M sodium phosphate buffer (PB, pH 7.4). The brains were removed and immersed them in 4% paraformaldehyde in 0.1 M PB for 24 hr at 4°C for post-fixation. The brains were kept in 30% sucrose in phosphate buffered saline (PBS) at 4°C for cryoprotection and frozen in cryostat embedding medium at -70°C (frozen section compound, Leica, Wetzlar, Germany). For immunostaining, brains were cryosectioned to 20  $\mu\text{m}$  sections on a cryostat (HM 525, Thermo Scientific, Waltham, MA, USA). Slices were washed three times with PBS, then incubated them in 3% methanol (MeOH).

The sectioned were incubated slides in 4% bovine serum albumin (BSA, Thermo Scientific) in PBS for 1 hr at room temperature, and thereafter with the rabbit polyclonal anti-CB1R antibody (1:200, Abcam, Cambridge, UK) diluted in 1% BSA with PBS overnight at 4°C. The following day, The slices were washed three times with Tris-buffered saline (TBS) with 1% Tween-20 for 5 min before incubating slices in the biotinylated anti-rabbit secondary antibody (1:200, Vector Laboratories, Burlingame, CA, USA) for 2 hr at room temperature. Sections were then rinsed and incubated them with avidin-biotinylated horseradish peroxidase complex (1:50, Vector Laboratories) in 0.3% PBS for 1 hr. After incubation, sections were then washed three times for 10 min and visualized CB1R by incubating for 5 min in a solution containing 3,3'-diaminobenzidine tetrahydrochloride (DAB), peroxidase substrate (0.1% of DAB, 0.1% ammonium nickel sulfate, and 0.01% H<sub>2</sub>O<sub>2</sub>, DAB substrate kit, Vector laboratories). Finally, the sections were washed to stop the DAB reaction, then dehydrated sections in ascending ethanol solutions, cleared sections in xylene, and all slides were cover-slipped using Permount (Fisher Scientific, Waltham, MA, USA).

The distribution of CB1Rs were determined in the IC according to the Paxinos & Watson's atlas of the rat brain.<sup>37</sup> Sections were evaluated with a binocular microscope and captured images using a digital camera (Olympus Inc., Melville, NY, USA). All CB1Rs images were quantified from light-field microscopy (40× objective, Olympus BX40, Olympus, Tokyo, Japan) with Image J. The numbers of counted CB1R were averaged from four sections for each animal.

## 5. Western blot

For insular cortices collection, animals were deeply anesthetized with isoflurane and decapitated them. The ipsilateral and contralateral insular cortices were isolated and transferred the brain regions into liquid nitrogen. For protein extraction, the isolated tissues were homogenized in lysis buffer (iNtRON Biotechnology Inc., Seongnam, Korea). The homogenate was centrifuged at 22,250 g for 10 min at 4°C, and the supernatant layer was separated from the pellet. The total protein concentrations of lysates were assessed with a spectrophotometer (ND-1000, NanoDrop Technologies Inc.,

Wilmington, DE, USA) and separated 15  $\mu$ g of protein by 10% sodium dodecyl sulfate polyacrylamide gel electrophoresis (SDS-PAGE). Proteins were transferred onto polyvinylidenedifluoride (PVDF) membranes (GE Healthcare, Buckinghamshire, UK), blocked membranes in 4% skim milk in TBS with Tween-20 (TBS-T) for 1 hr at room temperature, and incubated overnight at 4°C with either rabbit polyclonal primary antibody to FAAH, NAPE-PLD, CB1R, CB2R (1:200, Cayman Chemicals, Ann Arbor, MI, USA), or GAPDH (1:10,000, Ab Frontier, Seoul, Korea). The following day, blots were washed in TBS-T buffer and incubated with horseradish peroxidase (HRP)-conjugated polyclonal anti-rabbit IgG (1:5000, Abcam, Cambridge, UK). Immunoreactivity was visualized using a chemiluminescent substrate (ECL Prime western blotting detection reagent, GE Healthcare) and processed with a local allocation system (ImageQuant LAS 4000 Mini, GE Healthcare). Protein levels were normalized with respect to the signals obtained with anti-GAPDH antibody.

## 6. Quantative real-time PCR

### A. RNA extraction and cDNA synthesis

Approximately 30 mg of frozen tissues were homogenized in 1 ml of RiboEX solution (Geneall Biotechnology, Seoul, Korea) according to the manufacturer's instructions. The purity and concentration of total RNA were measured with a spectrophotometer (ND-1000, NanoDrop Technologies Inc.,) at 260 nm ( $A_{260}$ ) and 280 nm ( $A_{280}$ ). Using the SYBR® PrimeScript™ miRNA RT-PCR Kit (TaKaRa), the reverse transcription reaction of total RNA was performed with oligodT primer SuperScript III RT (TaKaRa), according to the manufacturer's protocols under the following conditions: 60°C for 60 min, followed by 85°C for 5 s.

### B. SYBR-Green quantative real-time PCR

Quantitative PCR was done on a CFX96 detection system (CFX96; Bio-Rad, USA).

SYBR® Premix Ex Taq™ II (TaKaRa, Dalian, China) was measured to measure the relative gene expression in cDNA samples from the sham-operated, neuropathic pain, and URB597-treated groups. The PCR mixture contained 10 µl of SYBR® Premix Ex Taq™ II, 0.4 µl of ROX solution, 1 µl of specific primer, 1 µl of RT reaction solution, and 5.6 µl of dH<sub>2</sub>O. The quantitative PCR was done with primers specific for NAPE-PLD, CB1R, CB2R, FAAH, and TRPV1, under the following conditions: 95°C for 30 min, followed by 40 cycles of 95°C for 5 s and 60°C for 20 s. After PCR, the amplification and melting curves were checked, calculated the mRNA concentration with software (Bio-Rad CFX Manager, Hercules, CA, USA), and represented as mean  $2^{-\Delta\Delta CT} \pm$  standard deviation (SD). Average Ct values were normalized to average Ct values for GAPDH mRNA from the same cDNA preparations. Results presented are expressed as fold increases over control values. The following primers were used: FAAH (Reverse: 5'-TCCACTGGGCAATCACAGAC-3', Forward: 5'-CAGTATGCGTCCTCGGTCAG-3'); NAPE-PLD (Reverse: 5'-TCAAGCTCCTCTTTGGAACCC-3', Forward: 5'-CATGGCCAACGTGGAAGAAC-3'); CB1R: (Reverse: 5'-GGAGGGAACCCTCAGCCAT-3', Forward: 5'-GGAGAACTTACTGTGAACAGGC-3'); GAPDH (Reverse: 5'-GGTGGTGAAGACGCCAGTAG-3', Forward: 5'-CACCATCTTCCAGGAGCGAG-3').

## 7. Statistical Analysis

Data are presented as means  $\pm$  standard error of the mean (SEM). Statistical significance was determined using the unpaired *t* tests between groups, one-way analysis of variance (ANOVA) with Dunnett's post-hoc analysis, or two-way ANOVA with Bonferroni's post-hoc analysis. In all cases, P-values <0.05 were considered significant.

### III. RESULTS

#### 1. Peripheral nerve injury leads to the development of mechanical allodynia

The time dependent behavioral changes were examined in neuropathic rats by measuring mechanical threshold at 1, 4, 7, and 14 days after neuropathic pain surgery. The mechanical threshold of the neuropathic pain (NP) group was significantly lower than that of the sham-operated group on POD1 ( $P<0.05$ ), POD4 ( $P<0.001$ ), POD7 ( $P<0.001$ ), and POD14 ( $P<0.001$ ) (two-way repeated measured ANOVA followed by Bonferroni's multiple comparison,  $n=7$ , Figure 2).<sup>39</sup>

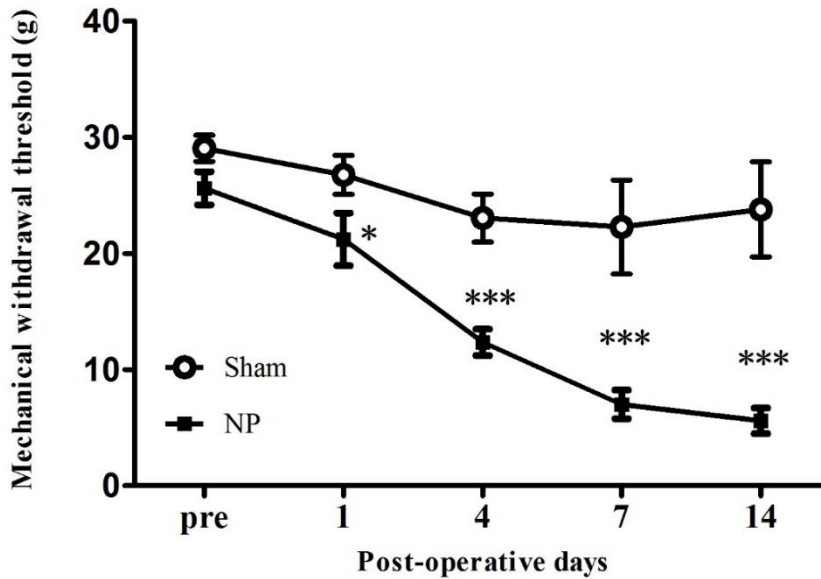


**Figure 2. Development of mechanical allodynia in neuropathic pain rats and sham-operated rats.** After nerve injury, animals developed significant mechanical allodynia on postoperative day 1 (POD1), POD4, POD7, and POD14 compared with the sham-operated group. Data are presented as means  $\pm$  standard error of mean (SEM). \* $P < 0.05$  and \*\*\* $P < 0.001$  were considered statistically significant. Two-way repeated ANOVA, followed by Bonferroni's post-hoc multiple comparison test. Neuropathic pain, NP.

## 2. Neuropathic pain activates FAAH signaling-related factors in the IC

To determine whether nerve injury can cause FAAH-related molecular changes, mRNA expression levels of FAAH signaling-related proteins CB1R, NAPE-PLD, FAAH, and TRPV1 were measured in the IC 14 days after nerve injury. The results indicate that on POD14, mRNA levels were upregulated for CB1R, NAPE-PLD and TRPV1 in the NP group (n=6) compared with mRNA levels of these proteins in the sham group (n=6,  $P < 0.05$ , Figure 3). However, no differences were found in FAAH levels (Figure 3C). These results suggest that the FAAH signaling pathway in the IC is strongly related to neuropathic pain.

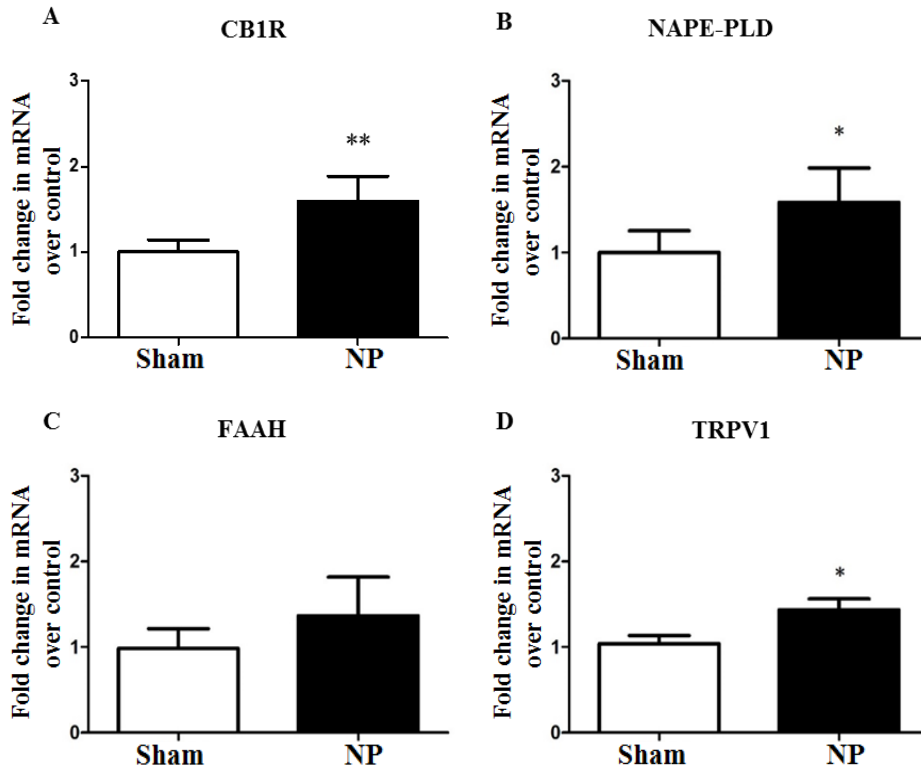


**Figure 3. mRNA expression of CB1R, NAPE-PLD, and TRPV1 increases in the IC of neuropathic pain rats compared with sham-operated rats.** Quantitative reverse transcription polymerase chain reaction (RT-PCR) was used to measure (A) CB1R, (B) NAPE-PLD, (C) FAAH, and (D) TRPV1 mRNA in the IC of the neuropathic pain (NP) group (n=6) and the sham group (n=6). CB1R, NAPE-PLD, and TRPV1 mRNA were significantly up-regulated in the nerve injury group compared with the sham-operated group, but the level of FAAH was not significantly different between NP and sham-operated groups. The results are presented as a fold change normalized to GAPDH expression. Data are presented as mean  $\pm$  standard error of mean (SEM) Asterisks indicate significance compared with sham group; \*  $P < 0.05$ , \*\*  $P < 0.01$ , unpaired  $t$  test

### 3. Expression of FAAH signaling-related proteins in the IC after nerve injury

To further investigate protein alterations related to FAAH signaling in the IC resulting from neuropathic pain, protein levels in the IC of CB1R, NAPE-PLD, FAAH, and TRPV1 were measured 14 days after nerve injury (n=7, each groups,  $P<0.05$ , Figure 4). Neuropathic pain derived from peripheral nerve injury caused significantly elevated levels of CB1R, NAPE-PLD, and TRPV1 (Figure 4A, B, and D), although there was no change in the FAAH level (Figure 4C). It is noteworthy that increased CB1R and TRPV1 expression in the IC of neuropathic pain rats may contribute to the analgesic efficacy of inhibiting FAAH activity.

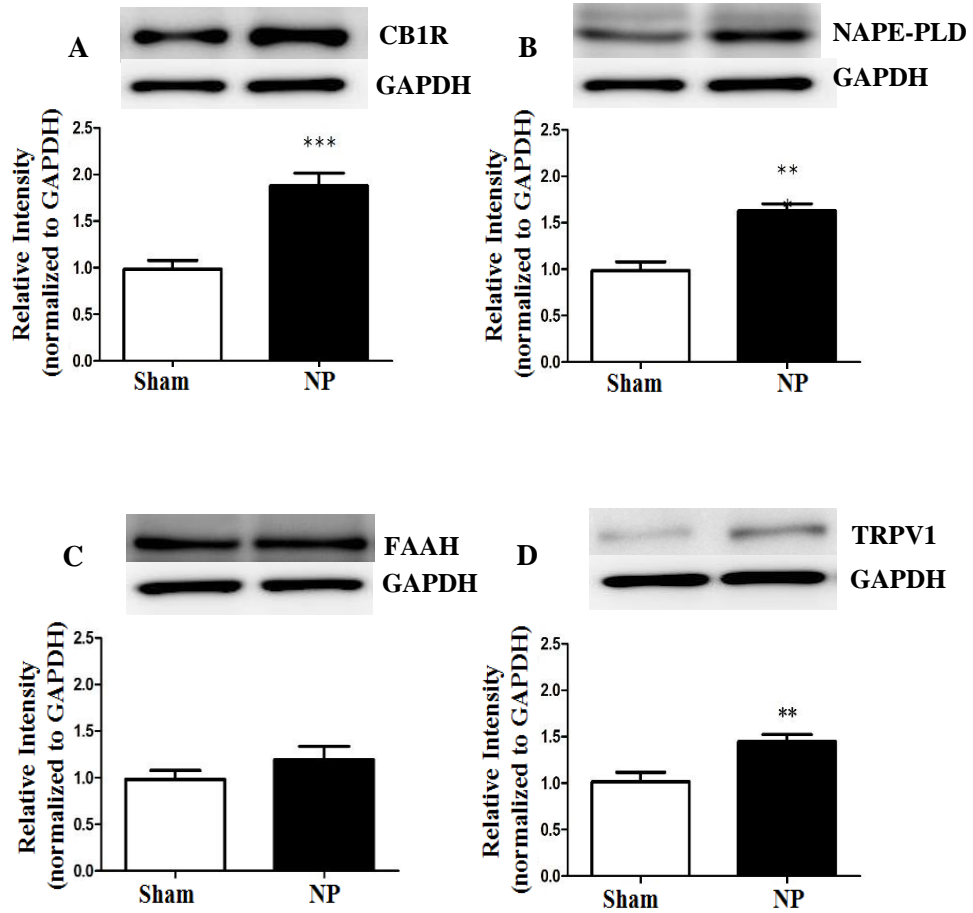


**Figure 4. Changes in expression levels of FAAH-related protein in the IC of NP groups compared with sham groups.** The protein expression of (A) CB1R, (B) NAPE-PLD, and (D) TRPV1 in the IC of the NP group (n=6) and sham group (n=6). CB1R, NAPE-PLD, and TRPV1 expression were upregulated in the nerve injury group compared with the sham-operated group, but the level of FAAH was not significantly different between NP and sham-operated groups. Representative images of western blot bands are shown with GAPDH as a loading control. Data are presented as mean  $\pm$  standard error of mean (SEM). Asterisks indicate significance compared with sham group; \*\*  $P < 0.01$ , \*\*\*  $P < 0.001$ , unpaired *t* test.

#### 4. URB597 microinjection into the IC reduces mechanical threshold

Previous studies demonstrated that systemic or intrathecal administration of URB597 reduces neuropathic pain<sup>40</sup>; however, it is unknown if URB597 administration directly to the IC reduces pain. Therefore, here the effects of URB597 were investigated in the IC of a rat model of neuropathic pain. The dose-dependent effects of this FAAH inhibitor on mechanical threshold were examined 14 days after nerve injury surgery (Figure 5). The behavioral changes were tested in four groups: 1 nM, 2 nM, and 4 nM URB597-microinjected neuropathic groups and the vehicle-treated neuropathic pain group. Before microinjection, the mechanical threshold were measured, then microinjections for the four treatment groups were administrated to the IC. Microinjection of the FAAH inhibitor, URB597, increased the mechanical threshold. Between 0.5 and 2 hr, this effect was significant at doses of 2 nM and 4 nM of URB597, but not at a 1 nM dose or with the vehicle treatment (Figure 5,  $P < 0.001$ ,  $n = 7$  each, two-way repeated measured ANOVA followed by Bonferroni's multiple comparison). The time course for mechanical threshold in the URB597-injected groups ( $n = 7$ ) shows that the anti-allodynia effect of URB597 lasts 4 hr after injection. However, animals injected with vehicle alone showed no significant change in mechanical threshold ( $P > 0.05$ ) at any time point.

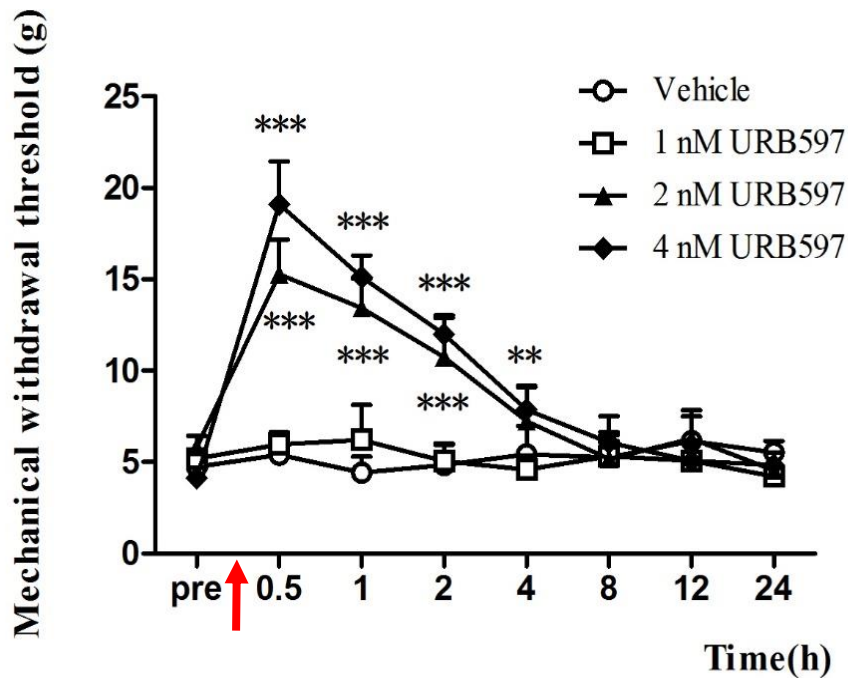


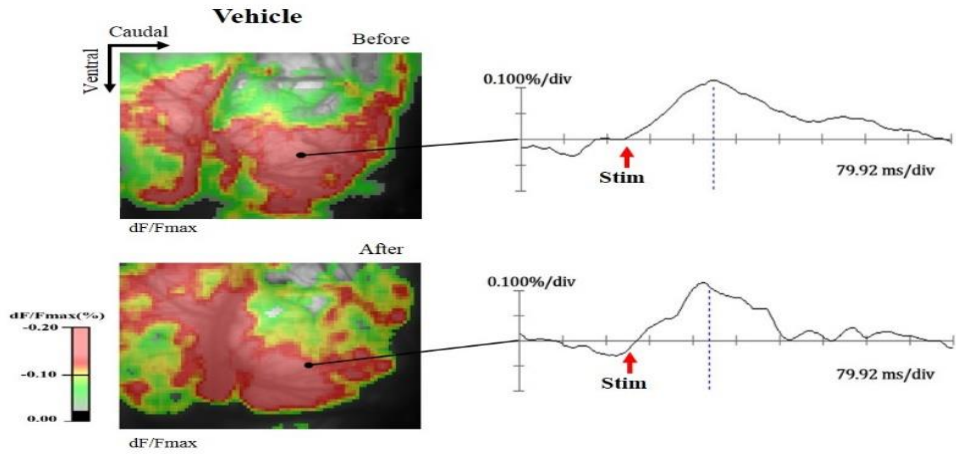
**Figure 5. Microinjection of URB597 attenuates mechanical allodynia in a dose-dependent manner.** Changes in paw withdrawal thresholds in response to mechanical stimulation after microinjection of URB597 or vehicle on POD14. The arrow indicates the time point of microinjection. Significant differences in withdrawal threshold between 2 nM or 4 nM URB597 and vehicle-treated groups were observed between 0.5 hr and 4 hr after microinjection. The most prominent changes in withdrawal threshold were observed in the 4 nM URB597-treated group, with significant changes observed between 0.5 hr and 4 hr after microinjection. Data are represented as means  $\pm$  standard error of mean (SEM);  $n=7$  rats/group,  $**P<0.01$ ,  $***P<0.001$  was considered statistically significant. Two-way repeated measure analysis of variance (ANOVA), followed by Bonferroni's post-hoc multiple comparison test.

## 5. Inhibition of FAAH by URB597 reduces IC excitability during neuropathic pain

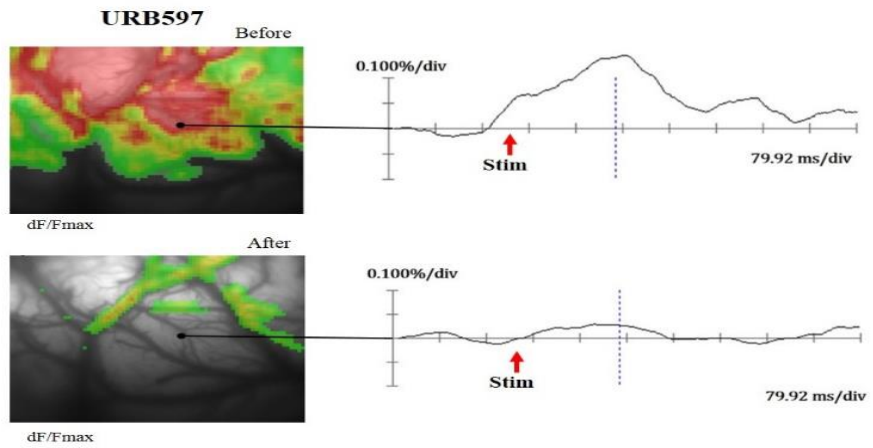
Optical signals in the IC increased in the nerve-injured rats after peripheral electrical stimulation. Representative optical images were obtained by electrical stimulation (5 mA) of the contralateral hind paw in nerve-injured rats before and after drug treatment (Figure 6). Wave forms represent the optical responses at specific points in each image of the IC. Figure 6A and B are representative images before and after treatment with either vehicle or 4 nM URB597. No significant difference was found for before and after vehicle treatment. Surprisingly, the optical activation of the IC was lower after URB597 treatment than before the treatment.

Peak amplitudes and activated areas of the IC are represented in Figure 6C and 6D, respectively. The peak amplitudes evoked by 5.0 mA peripheral electrical stimulation of neuropathic rats were reduced after URB597 treatment compared to before the treatment (Figure 6C;  $n=6$ ,  $P<0.01$ ). The activated areas corresponding to electrical stimulation in neuropathic rats decreased after URB597 treatment, compared to before treatment (Figure 6D;  $n=6$ ,  $P<0.01$ ). However, no significant differences in peak amplitudes or activated areas was found for before and after vehicle treatment in the IC of neuropathic rats (Figure 6C and D).

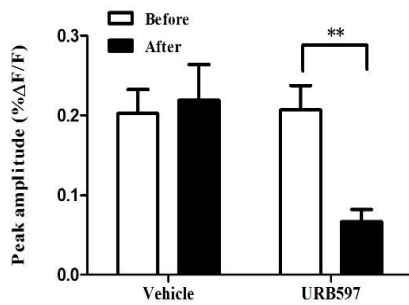
**A**



**B**



**C**



**D**

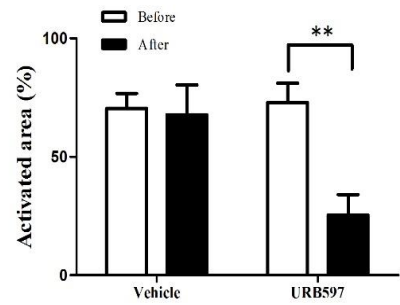


**Figure 6. Changes in optical signals of the IC before and after treatment with 4 nM URB597 or vehicle in nerve-injured rats.** (A) Optical images before and after the vehicle treatment in a nerve-injured rat and (B) Optical images before and after the 4 nM URB597 treatment in a nerve-injured rat. The activated area was color-coded, and the data from optical signals are represented as the percent change in fluorescent intensity ( $\% \Delta F/F$ ). (C) Peak amplitudes before and after treatments with vehicle or URB597 in response to 5.0 mA electrical stimulation of the left hind paw in nerve-injured rats. (D) Activated area before and after treatments with vehicle or 4 nM URB597 treatment in response to 5.0 mA electrical stimulation of the left hind paw in nerve-injured groups. The peak amplitudes and activated areas induced by peripheral electrical stimulation after 4 nM URB597 treatment were significantly lower than those before URB597 treatment. The arrow indicates the electrical stimulation applied to the hind paw at 0 ms. However, there were no significant changes in peak amplitudes and activated areas before and after vehicle treatment. Data are presented as mean  $\pm$  standard error of mean (SEM). \*\* $P < 0.01$ . Unpaired  $t$  test for post-hoc comparisons between groups.

## 6. Inhibition of FAAH reduces neuronal activation related to IC pain

To further confirm enhanced cortical activity in response to neuropathic pain, c-Fos expression in the IC was examined using immunohistochemistry. As shown in Figure 7, the number of cells positive for c-Fos in the IC increased 14 days after induction of neuropathic pain, compared with sham-operated groups (Figure 7A and B). The NP rats had a higher number of c-Fos-positive cells and rats receiving 4 nM URB597 injections on POD14 had lower numbers of c-Fos positive cells (Figure 7A, photomicrographs and Figure 7B, graph of c-Fos positive cells,  $n=6$  each group,  $P<0.05$ , unpaired  $t$  test). These results indicate that neuronal activity of IC is enhanced in response to neuropathic pain and is also attenuated by FAAH inhibition.

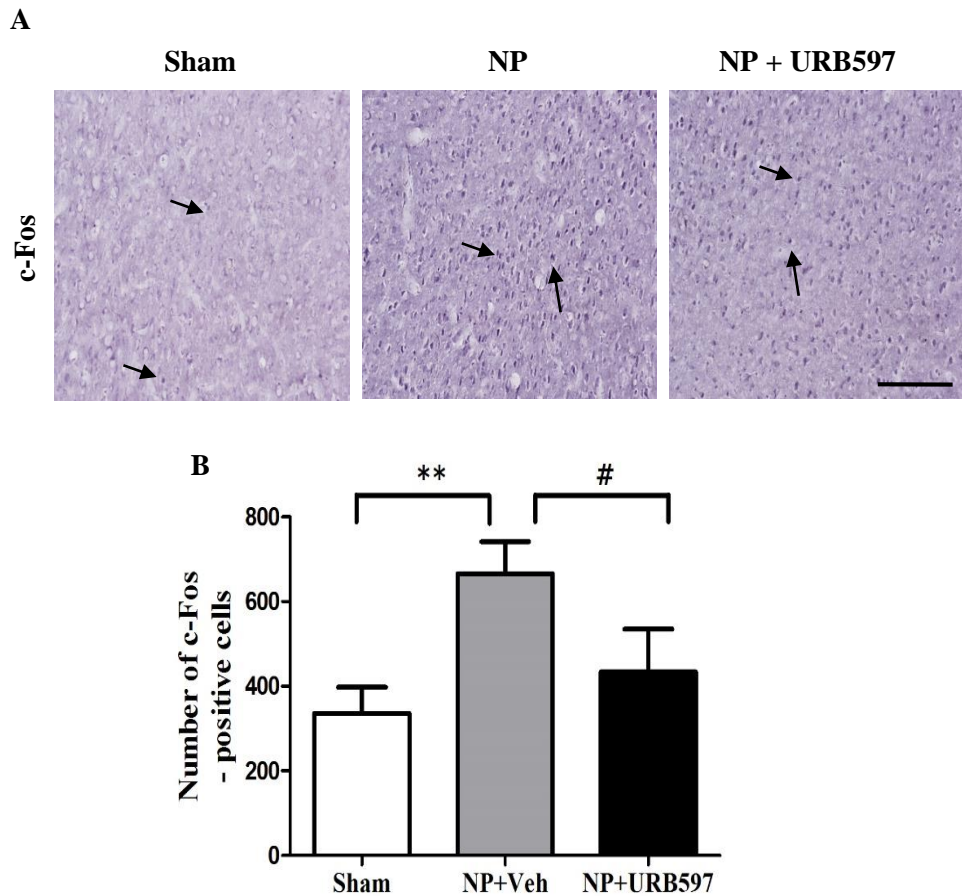


**Figure 7. Changes in c-Fos expression after microinjection of URB597 in the IC.** (A) Representative photomicrographs of c-Fos-positive cells in the IC. The arrows indicate c-Fos-positive cells on POD14. (B) Number of c-Fos-positive cells in the IC of sham-operated, vehicle-treated, and 4 nM URB597-treated groups on POD14. The c-Fos expression was significantly higher in the vehicle-treated group than sham-operated group. After microinjection of 4 nM URB597, the number of c-Fos-positive cells decreased in the IC of NP rats. Scale bars, 200 $\mu$ m. Data are presented as means  $\pm$  standard error of mean (SEM), \*\* $P < 0.01$ , vs. Sham. # $P < 0.05$  vs. NP+4 nM, One-way ANOVA followed by Dunnett's post-hoc multiple comparison test.

## 7. Nerve injury elevates CB1R in the insular cortex

Previous studies have shown that the IC is important for modulating the sensory components of pain.<sup>41</sup> To elucidate the involvement of the IC in the anti-allodynic effects of URB597, immunohistochemistry was used to examine whether microinjected URB597 had detectable effects in the IC region. Histological imaging was performed 30 mins after injection of 4 nM URB597 or vehicle. On POD14, expression of CB1Rs were observed by marked dark staining and arrows in the IC of NP rats. The number of CB1R-positive cells were found on POD14 in the nerve-injured group was significantly higher than in the sham-operated group (Figure 8A, second lane photomicrographs and Figure 8B, graph of CB1R-positive cells, n=6 per groups,  $P<0.01$ ,  $P<0.001$ ). However, expression of CB1R after the 4 nM URB597 treatment was not significantly different than for the vehicle treatment alone (Figure 8).

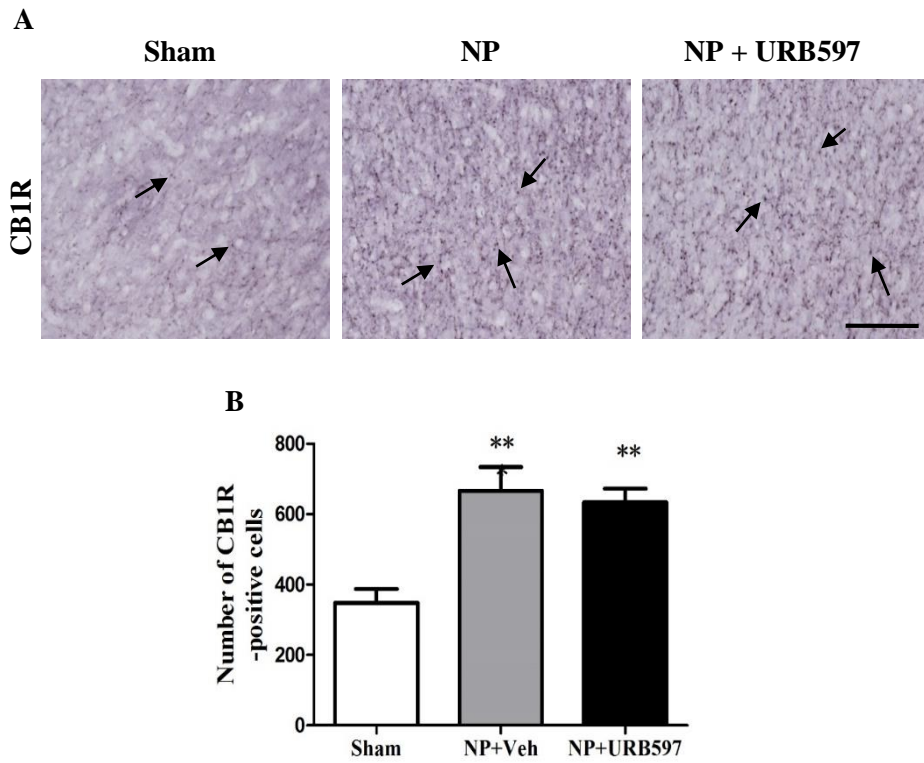


**Figure 8. Changes in CB1R in the IC after microinjection of 4 nM URB597 or vehicle in the neuropathic pain rats.** (A) Photomicrographs of CB1R-positive cells in the IC. Arrows indicate CB1R-positive cells on POD14. (B) Numbers of CB1R-positive cells in the IC of sham-operated, vehicle-treated, and 4 nM URB597-treated groups on POD14. The expression of CB1R increased significantly after nerve injury, compared with the sham-operated group. However, microinjection of 4 nM URB597 did not change CB1R expression in the IC. Scale bars, 400 $\mu$ m. Data are presented as means  $\pm$  standard error of mean (SEM). \*\*P<0.01, \*\*\*P<0.001 vs. Sham, One-way analysis of variance (ANOVA) followed by Dunnett's post-hoc multiple comparison test.

## 8. Microinjection of URB597 into the IC increases levels of NAPE-PLD.

Western blot was performed to determine whether intracranial administration of URB597 would affect the FAAH signaling pathway, specifically the proteins CB1R, NAPE-PLD, FAAH, and TRPV1, which are well known to be activated by the endocannabinoid ligand AEA.<sup>42</sup> One-way ANOVA analysis of neuropathic pain rats showed significantly higher NAPE-PLD protein expression in the 2 nM and 4 nM URB597 injection groups than a vehicle-treated group (Figure 9A,  $P < 0.01$ ). However, protein expression of other FAAH signaling components did not significantly change after URB597 microinjection. Specifically, the levels of CB1R (Figure 9A,  $P > 0.05$ ), FAAH (Figure 9C,  $P > 0.05$ ), and TRPV1 (Figure 9D,  $P > 0.05$ ) did not change in rats receiving different doses of URB597 or a vehicle treatment.

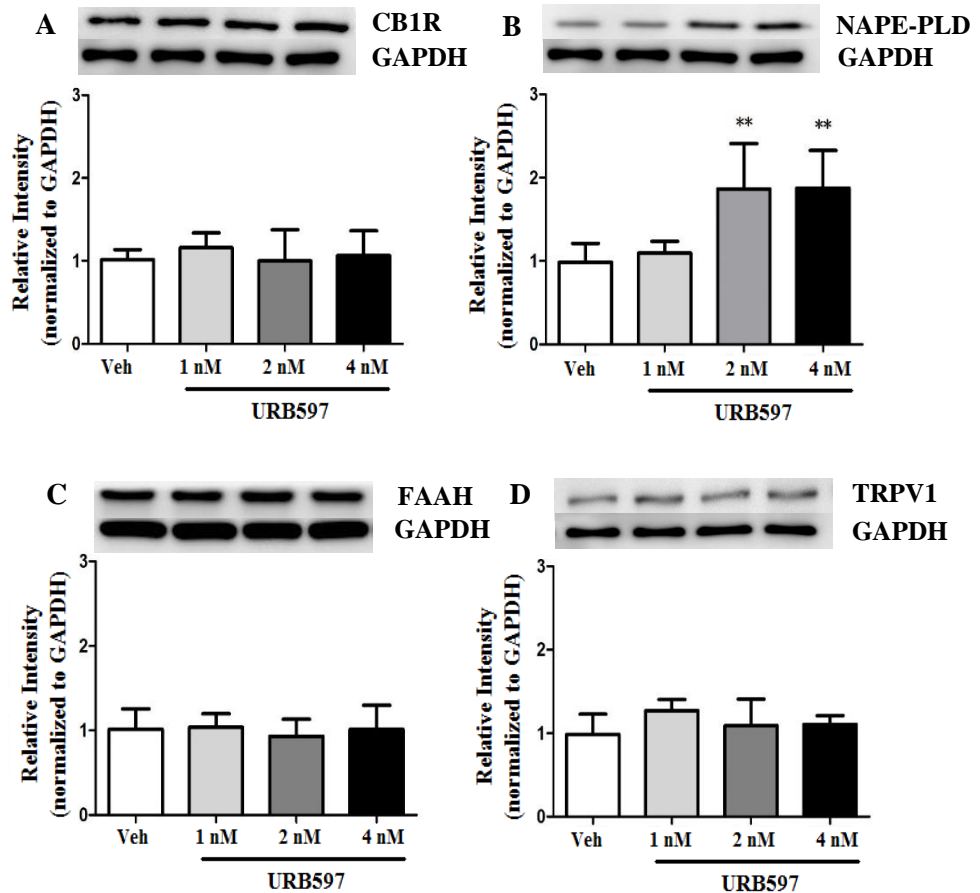


**Figure 9. Effects of URB597 on the expression of CB1R, NAPE-PLD, FAAH, and TRPV1 in the IC.** The expression levels of (A) CB1R (B) NAPE-PLD (C) FAAH and (D) TRPV1 after microinjection of URB597. Levels of NAPE-PLD were significantly increased in the 2 nM and 4 nM URB597-treated groups compared with the vehicle-treated group. Levels of CB1R, FAAH, and TRPV1 were similar among groups. Representative images of western blots are shown with GAPDH as a loading control. Histogram represents the mean  $\pm$  standard error of mean (SEM) of quantified western blot band intensities (n=7/group). \*\*P<0.01, vs. vehicle-treated group. One-way ANOVA followed by Dunnett's post-hoc multiple comparison test.

## 9. mRNA expressions of endocannabinoid components

To address whether the changes in FAAH signaling-related components after URB597 microinjection into the IC were associated with a nerve-injured states, the gene expression of CB1R, NAPE-PLD, FAAH, and TRPV1 in the IC were analyzed. Similar to western blot data, data shows that only mRNA levels of NAPE-PLD changed in the 4 nM URB597-treated group (Figure 10B,  $P < 0.001$ ). Other than NAPE-PLD, there were no significant changes in the gene expressions of other endocannabinoid related components (Figure 10A, C, and D,  $P > 0.05$ ).

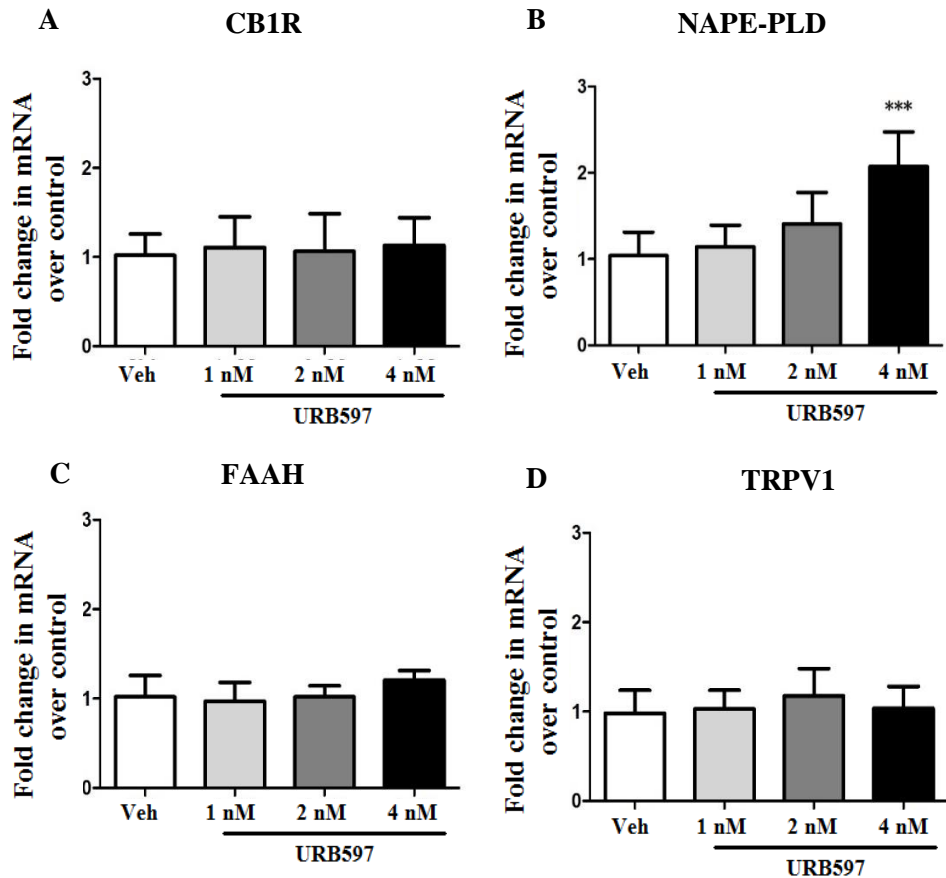


**Figure 10. Changes in mRNA levels of FAAH signaling component following URB597 microinjection into the IC.** (A) CB1R, (B) NAPE-PLD, (C) FAAH, and (D) TRPV1 gene expression levels in the IC after microinjection of vehicle or URB597 at 1 nM, 2 nM, or 4 nM. Level of NAPE-PLD was significantly increased in the 4 nM URB597-treated group compared with the vehicle-treated group. Levels of CB1R, FAAH, and TRPV1 in all groups did not change over doses. Data are presented as the mean  $\pm$  standard error of mean (SEM) (n=6/group). The results are presented as a fold change normalized to GAPDH expression. \*\*\*P<0.001, vs. vehicle-treated group. One-way ANOVA followed by Dunnett's post-hoc multiple comparison test.

#### IV. DISCUSSION

Many aspects of the mechanism for neuropathic pain remain unknown, despite extensive previous studies.<sup>43,44</sup> The present study provides integrated behavioral, electrophysiological, and biochemical evidence showing pain modulation via FAAH inhibition in the IC after peripheral nerve injury. It is known that increasing endocannabinoids by blocking FAAH has antinociceptive effects in neuropathic pain.<sup>45</sup> Consequently, an FAAH inhibitor may provide a novel strategy for anti-allodynic drugs. There have been no reports of FAAH signaling related to modulation of neuropathic pain. The selective FAAH inhibitor URB597 was used to inhibit FAAH activity in an animal model of neuropathic pain, and found that it suppressed neuropathic pain through the conservation of the endocannabinoid AEA in the IC.<sup>45-47</sup> This is the first to demonstrate potential anti-allodynic effects of URB597 in the IC and provide evidence that supports a pain modulation role for the FAAH signaling pathway in the IC.

Previous studies have shown that the IC has an important role in the pain modulation process<sup>5,48</sup> and consists of multiple neurotransmitter systems related to pain, including cannabinergic, opioidergic, serotonergic, and dopaminergic transmissions.<sup>49,50</sup> Moreover, previous studies showed a significant increase in both mRNA and protein expression levels of CB1R, TRPV1, and NAPE-PLD in the DRG of neuropathy rats during the development or maintenance of pain.<sup>51, 41</sup> Similarly, decrease in mechanical threshold was observed after nerve injury on POD14 and increase in mRNA and protein expression levels of CB1R, NAPE-PLD, and TRPV1 in the IC of nerve-injured rats. Such robust expression levels suggest that the modulation of neuropathic pain through changes of FAAH signaling-related factors is evident in the IC.

URB597, an FAAH inhibitor, reduces the nociceptive response caused by inflammatory and neuropathic pain via the systemic or intrathecal administration<sup>40</sup> and these pain-relieving effects can be blocked by using cannabinoid receptor antagonists.<sup>52,53</sup> In this study, changes in mechanical threshold were observed after direct injection of the FAAH inhibitor into the IC of peripheral nerve-injured rats. In particular, microinjection of URB597 at doses of 2 nM and 4 nM significantly reduced mechanical allodynia on POD14. However, the analgesic effect did not persist for 8 hr after injection. Thus, these results suggest that URB597 reduces pain-related behaviors by inhibiting the activation

of FAAH.

Distinct changes in neuronal activation were found under neuropathic pain conditions after URB597 treatment in the IC, by performing an electrophysiological study to examine neuronal excitation induced by neuropathic pain and studying the inhibitory effects of URB597 on pain signals. Previous study presented a visualization of neuronal excitation in the IC after peripheral nerve injury.<sup>38, 54</sup> Thus, to examine changes in excitatory patterns in the IC between the neuropathic group and URB597-treated group, neuronal signals were recorded induced by electrical stimulation of the left hind paw. It is observed that neuronal activities increased in the peripheral nerve injury group and the inhibition of neuronal activities in the IC of neuropathic rats by URB597 treatment. In other words, excitability in the IC after nerve injury decreased after treatment with an FAAH inhibitor. Moreover, it is found that the increase of neuronal activity coincided with elevated c-Fos expression, an immediate early marker of neuronal activation.<sup>55,56</sup> The Expression of c-Fos increased after nerve injury and decreased after URB597 microinjection in the IC. These results indicates that the IC is closely related to nociception information processing and URB597 could reduce the response to peripheral nerve injury in the IC.

A previous study reported increased CB1R mRNA expression in the dorsal root ganglion<sup>41</sup> and spinal cord neurons<sup>57</sup> after nerve injury. It is found increased expression of both CB1R mRNA and protein, as well as increase in CB1R-positive cells in the IC 14 days after peripheral nerve injury. The increase in CB1R expressions results in augmented potency or efficacy of the up-regulated levels of AEA.<sup>58</sup> It is also likely that increased CB1R expression contributes to the effectiveness of AEA, providing relief from painful neuropathy symptoms after inhibition of FAAH. Besides, Neuropathic pain can induce synaptic plasticity and long-term potentiation (LTP) involved in the glutamatergic systems of the IC.<sup>59,60</sup> In this sense, glutamate and GABA release can be modulated by AEA and CB1R in presynaptic terminals, and the activation of CB1R by increased AEA through the inhibition of FAAH may decrease synaptic transmission to prevent LTP.<sup>59</sup> Thus, URB597 may produce analgesic effects by activating CB1R and consequently inhibiting LTP.<sup>61,62</sup>

Many studies have shown that FAAH inhibition attenuates mechanical allodynia and thermal hyperalgesia in neuropathic pain models.<sup>35,63,64</sup> Also, NAPE-PLD synthesis in

tissues elevates AEA levels.<sup>65,66</sup> This activity may be interpreted as an endogenous defense mechanism against pain. Accordingly, it is observed that microinjection of 2 nM and 4 nM URB597 increased NAPE-PLD expression in the IC of nerve-injured rats. The analgesic effect of AEA produced by NAPE-PLD in neuropathic conditions is difficult to observe, because AEA is immediately degraded by FAAH.<sup>45</sup> Although FAAH is the dominant enzyme that metabolizes AEA in the brain,<sup>67</sup> it is unknown how the metabolic pathways of FAAH signaling in the IC contribute to neuropathic pain. Besides its role in activating cannabinoid receptors,<sup>22,68</sup> AEA also activates TRPV1 receptors, which may lead to painful, burning sensations.<sup>57</sup> It is possible that elevating AEA levels by FAAH inhibition can cause simultaneous activation of conflicting mechanisms of cannabinoid receptors and TRPV1 to suppress or induce pain, respectively.

Here, this study provides possible evidence that inhibition of FAAH contributes to analgesic effects induced by increasing the expression of NAPE-PLD. As mentioned above, AEA which is synthesized by NAPE-PLD, activates CB1R, CB2R, and TRPV1. In this study, it is confirmed that TRPV1 is present in the IC by western blot and qPCR analysis. According to a previous study,<sup>42</sup> AEA activates CB1R after URB597 injection and may increase levels of NAPE-PLD protein or mRNA expression via TRPV1 activity. It is assumed that concentration of calcium ion in postsynaptic neurons is increased by the pain signal-induced release of glutamate in the presynaptic neurons, thereby synthesizing more NAPE-PLD that produces AEA.<sup>57,69</sup> AEA may then be released to the synaptic cleft from postsynaptic neurons via a membrane transporter, thus activating CB1R that is present in the presynaptic neurons.<sup>41,65</sup> Consequently, the influx of calcium ions in the presynaptic neurons is blocked by CB1R activation, preventing the release of glutamate. Because NAPE-PLD synthesis is dependent on the calcium ion concentration,<sup>14</sup> the expression of NAPE-PLD may decrease due to a glutamate release that is inhibited by the reduction of pain. However, elevated NAPE-PLD expression was found, which may indicate that AEA activates TRPV1 channels and subsequently increases calcium ion concentration. Although the activity of TRPV1 is known to sustain and induce pain,<sup>70</sup> the calcium ion influx mediated by this channel in the cannabinoid signaling pathway may prompt NAPE-PLD synthesis, which leads to the production of AEA, to reduce pain behavior (Figure 11).<sup>71</sup>

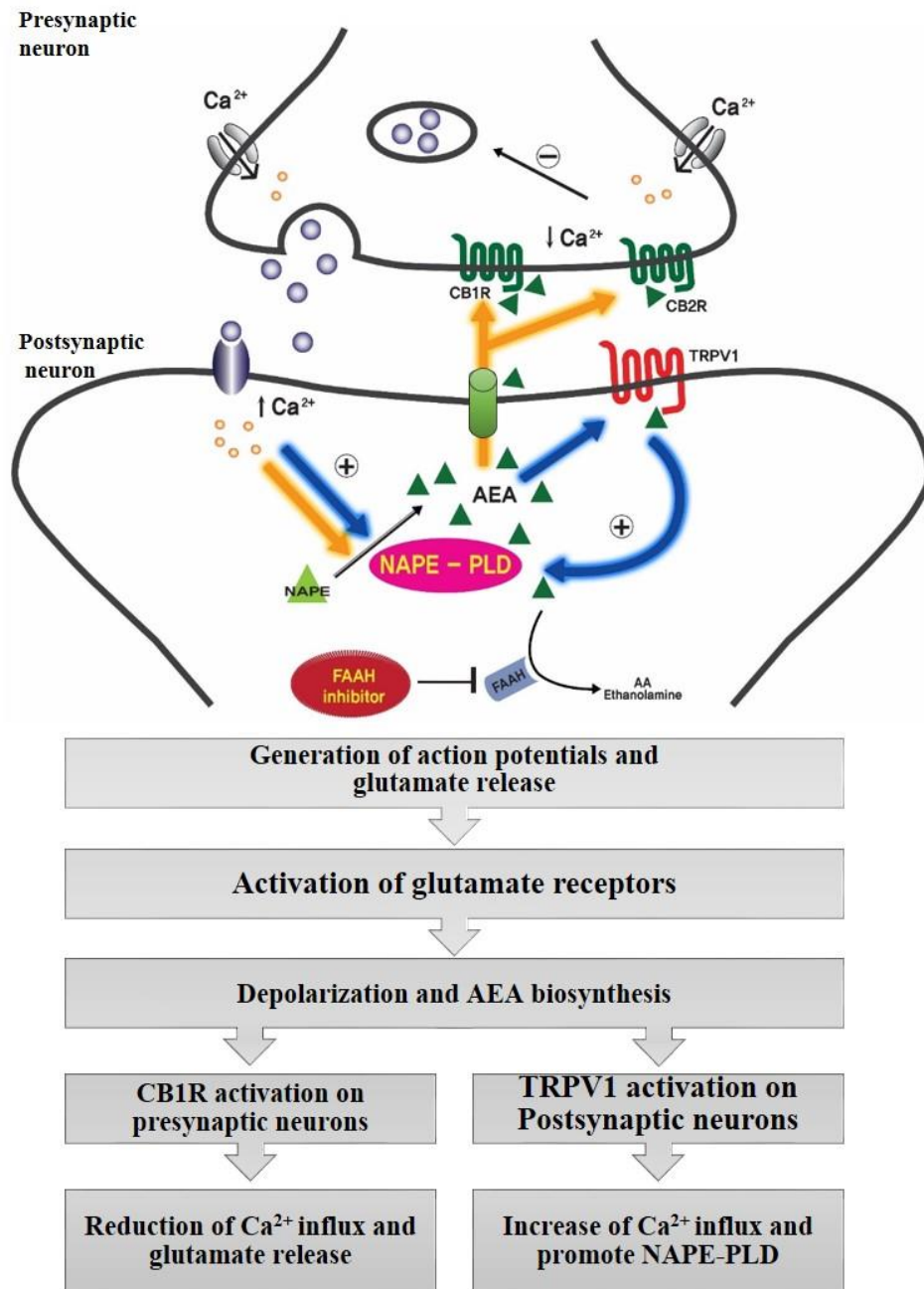


**Figure 11. Schematic representation of possible synaptic mechanisms of action for AEA in neurons in the IC.** The mechanisms by which AEA regulates synaptic transmission onto presynaptic and postsynaptic neurons are illustrated. AEA is produced

on demand by the  $\text{Ca}^{2+}$ -dependent enzymes NAPE-PLD respectively. Increases in intracellular  $\text{Ca}^{2+}$  can be prompted NAPE-PLD synthesis. When AEA levels are pharmacologically elevated by blocking its degradation by FAAH (using the FAAH-selective inhibitor URB597), AEA is able to activate metabotropic pre-synaptic CB1R and post-synaptic TRPV1 receptors. Stimulation of presynaptic CB1R reduces the release of stored neurotransmitters by inwardly closing  $\text{Ca}^{2+}$  channels (yellow-colored arrows). AEA biosynthesis may be triggered by activation of TRPV1 in postsynaptic neurons with subsequent  $\text{Ca}^{2+}$  entry which leads to synthesis of NAPE-PLD (blue-colored arrows).

There have been limited studies on the cannabinoid signaling pathway in the IC, but this region is shown to be involved in processing pain signals. Furthermore, future work involving measurement of AEA levels in the context of FAAH inhibition would reinforce this results. For further studies, it is suggested that CB2R, other TRP channel subfamilies, and COX-2 signaling to be considered for developing more effective pain control. Through this study, insights on a potential potent therapeutic target for managing neuropathic pain and lay groundwork for future studies are provided to extend this understanding of neuropathic pain. This study shows that peripheral nerve injury-related neuropathy is linked to FAAH signals in the IC. Direct administration of URB597 to the IC inhibits allodynia and the excitation of neurons in the IC. These results suggest that URB597 may provide an alternative therapeutic target to modulate neuropathic pain.

## V. CONCLUSION

In conclusion, URB597 has a key role as a potent analgesic agent when microinjected in the IC of neuropathic rats. This study shows that peripheral nerve-injured neuropathy may be sufficient to FAAH signals in the IC. Direct administration of URB597 proves to inhibit allodynia and excitation of neurons in the IC. These results suggest that URB597 may provide an alternative therapeutic target for the modulation of neuropathic pain.

## REFERENCES

1. Campbell JN, Meyer RA. Mechanisms of neuropathic pain. *Neuron* 2006;52:77-92.
2. Attal N, Cruccu G, Baron R, Haanpaa M, Hansson P, Jensen TS, et al. EFNS guidelines on the pharmacological treatment of neuropathic pain: 2010 revision. *Eur J Neurol* 2010;17:1113-e88.
3. Finnerup NB, Haroutounian S, Kamerman P, Baron R, Bennett DL, Bouhassira D, et al. Neuropathic pain: an updated grading system for research and clinical practice. *Pain* 2016;157:1599-606.
4. Attal N, de Andrade DC, Adam F, Ranoux D, Teixeira MJ, Galhardoni R, et al. Safety and efficacy of repeated injections of botulinum toxin A in peripheral neuropathic pain (BOTNEP): a randomised, double-blind, placebo-controlled trial. *Lancet Neurol* 2016;15:555-65.
5. Han J, Kwon M, Cha M, Tanioka M, Hong SK, Bai SJ, et al. Plasticity-Related PKMzeta Signaling in the Insular Cortex Is Involved in the Modulation of Neuropathic Pain after Nerve Injury. *Neural Plast* 2015;2015:601767.
6. Coghill R, Talbot J, Evans A, Meyer E, Gjedde A, Bushnell M, et al. Distributed processing of pain and vibration by the human brain. *The Journal of Neuroscience* 1994;14:4095-108.
7. Ploghaus A, Tracey I, Gati JS, Clare S, Menon RS, Matthews PM, et al. Dissociating Pain from Its Anticipation in the Human Brain. *Science* 1999;284:1979-81.
8. Peyron R, Schneider F, Faillenot I, Convers P, Barral FG, Garcia-Larrea L, et al. An fMRI study of cortical representation of mechanical allodynia in patients with neuropathic pain. *Neurology* 2004;63:1838-46.
9. Berthier M, Starkstein S, Leiguarda R. Asymbolia for pain: a sensory-limbic disconnection syndrome. *Ann Neurol* 1988;24:41-9.
10. Benison AM, Chumachenko S, Harrison JA, Maier SF, Falci SP, Watkins LR, et al. Caudal granular insular cortex is sufficient and necessary for the long-term maintenance of allodynic behavior in the rat attributable to mononeuropathy. *J Neurosci* 2011;31:6317-28.
11. Coffeen U, Manuel Ortega-Legaspi J, Lopez-Munoz FJ, Simon-Arceo K, Jaimes O, Pellicer F. Insular cortex lesion diminishes neuropathic and inflammatory pain-like behaviours. *Eur J Pain* 2011;15:132-8.
12. Starr CJ, Sawaki L, Wittenberg GF, Burdette JH, Oshiro Y, Quevedo AS, et al. Roles of the insular cortex in the modulation of pain: insights from brain lesions. *J Neurosci* 2009;29:2684-94.
13. Gaoni Y, Mechoulam R. Isolation, Structure, and Partial Synthesis of an Active Constituent of Hashish. *Journal of the American Chemical Society* 1964;86:1646-7.
14. Pertwee RG. Ligands that target cannabinoid receptors in the brain: from THC to anandamide and beyond. *Addict Biol* 2008;13:147-59.
15. Pertwee RG. The therapeutic potential of drugs that target cannabinoid receptors or modulate the tissue levels or actions of endocannabinoids. *Aaps j* 2005;7:E625-54.
16. Howlett AC, Barth F, Bonner TI, Cabral G, Casellas P, Devane WA, et al. International Union of Pharmacology. XXVII. Classification of cannabinoid receptors. *Pharmacol Rev* 2002;54:161-202.

17. Pertwee RG, Ross RA. Cannabinoid receptors and their ligands. Prostaglandins, Leukotrienes and Essential Fatty Acids (PLEFA) 2002;66:101-21.
18. Pertwee RG. Cannabinoid receptors and pain. Prog Neurobiol 2001;63:569-611.
19. Munro S, Thomas KL, Abu-Shaar M. Molecular characterization of a peripheral receptor for cannabinoids. Nature 1993;365:61-5.
20. Pertwee RG. Cannabinoids [Handbook of Experimental Pharmacology 168]. 2005.
21. Wotherspoon G, Fox A, McIntyre P, Colley S, Bevan S, Winter J. Peripheral nerve injury induces cannabinoid receptor 2 protein expression in rat sensory neurons. Neuroscience 2005;135:235-45.
22. Ross RA, Coutts AA, McFarlane SM, Anavi-Goffer S, Irving AJ, Pertwee RG, et al. Actions of cannabinoid receptor ligands on rat cultured sensory neurones: implications for antinociception. Neuropharmacology 2001;40:221-32.
23. Mechoulam R, Ben-Shabat S, Hanus L, Ligumsky M, Kaminski NE, Schatz AR, et al. Identification of an endogenous 2-monoglyceride, present in canine gut, that binds to cannabinoid receptors. Biochemical Pharmacology 1995;50:83-90.
24. Sugiura T, Kondo S, Sukagawa A, Nakane S, Shinoda A, Itoh K, et al. 2-Arachidonoylglycerol: A Possible Endogenous Cannabinoid Receptor Ligand in Brain. Biochemical and Biophysical Research Communications 1995;215:89-97.
25. Devane W, Hanus L, Breuer A, Pertwee R, Stevenson L, Griffin G, et al. Isolation and structure of a brain constituent that binds to the cannabinoid receptor. Science 1992;258:1946-9.
26. Tzavara ET, Li DL, Moutsimilli L, Bisogno T, Di Marzo V, Phebus LA, et al. Endocannabinoids activate transient receptor potential vanilloid 1 receptors to reduce hyperdopaminergia-related hyperactivity: therapeutic implications. Biol Psychiatry 2006;59:508-15.
27. Chiou L-C, Hu SS-J, Ho Y-C. Targeting the cannabinoid system for pain relief? Acta Anaesthesiologica Taiwanica 2013;51:161-70.
28. Di Marzo V, De Petrocellis L, Bisogno T. The biosynthesis, fate and pharmacological properties of endocannabinoids. Handb Exp Pharmacol 2005:147-85.
29. Sugiura T, Waku K. Cannabinoid receptors and their endogenous ligands. J Biochem 2002;132:7-12.
30. Di Marzo V. The endocannabinoid system: its general strategy of action, tools for its pharmacological manipulation and potential therapeutic exploitation. Pharmacol Res 2009;60:77-84.
31. Richardson JD, Aanonsen L, Hargreaves KM. Antihyperalgesic effects of spinal cannabinoids. Eur J Pharmacol 1998;345:145-53.
32. Helyes Z, Nemeth J, Than M, Bolcskei K, Pinter E, Szolcsanyi J. Inhibitory effect of anandamide on resiniferatoxin-induced sensory neuropeptide release in vivo and neuropathic hyperalgesia in the rat. Life Sci 2003;73:2345-53.
33. Rahn EJ, Hohmann AG. Cannabinoids as pharmacotherapies for neuropathic pain: from the bench to the bedside. Neurotherapeutics 2009;6:713-37.
34. Lichtman AH, Leung D, Shelton CC, Saghatelian A, Hardouin C, Boger DL, et al. Reversible inhibitors of fatty acid amide hydrolase that promote analgesia: evidence for an unprecedented combination of potency and selectivity. J Pharmacol Exp Ther 2004;311:441-8.
35. Kinsey SG, Long JZ, O'Neal ST, Abdullah RA, Poklis JL, Boger DL, et al. Blockade of endocannabinoid-degrading enzymes attenuates neuropathic pain. J Pharmacol

- Exp Ther 2009;330:902-10.
36. Leung D, Saghatelian A, Simon GM, Cravatt BF. Inactivation of N-Acyl Phosphatidylethanolamine Phospholipase D Reveals Multiple Mechanisms for the Biosynthesis of Endocannabinoids. *Biochemistry* 2006;45:4720-6.
  37. Paxinos G, Watson C. *The Rat Brain in Stereotaxic Coordinates*: Academic; 2007.
  38. Han J, Cha M, Kwon M, Hong SK, Bai SJ, Lee BH. In vivo voltage-sensitive dye imaging of the insular cortex in nerve-injured rats. *Neurosci Lett* 2016;634:146-52.
  39. Lee BH, Won R, Baik EJ, Lee SH, Moon CH. An animal model of neuropathic pain employing injury to the sciatic nerve branches. *Neuroreport* 2000;11:657-61.
  40. Yesilyurt O, Cayirli M, Sakin YS, Seyrek M, Akar A, Dogrul A. Systemic and spinal administration of FAAH, MAGL inhibitors and dual FAAH/MAGL inhibitors produce antipruritic effect in mice. *Arch Dermatol Res* 2016;308:335-45.
  41. Mitrirattanakul S, Ramakul N, Guerrero AV, Matsuka Y, Ono T, Iwase H, et al. Site-specific increases in peripheral cannabinoid receptors and their endogenous ligands in a model of neuropathic pain. *Pain* 2006;126:102-14.
  42. Horvath G, Kekesi G, Nagy E, Benedek G. The role of TRPV1 receptors in the antinociceptive effect of anandamide at spinal level. *PAIN* 2008;134:277-84.
  43. Gussew A, Rzanny R, Erdtel M, Scholle HC, Kaiser WA, Mentzel HJ, et al. Time-resolved functional 1H MR spectroscopic detection of glutamate concentration changes in the brain during acute heat pain stimulation. *Neuroimage* 2010;49:1895-902.
  44. Frot M, Faillenot I, Mauguier F. Processing of nociceptive input from posterior to anterior insula in humans. *Hum Brain Mapp* 2014;35:5486-99.
  45. Hama AT, Germano P, Varghese MS, Cravatt BF, Milne GT, Pearson JP, et al. Fatty acid amide hydrolase (FAAH) inhibitors exert pharmacological effects, but lack antinociceptive efficacy in rats with neuropathic spinal cord injury pain. *PLoS One* 2014;9:e96396.
  46. Peng X, Studholme K, Kanjiya MP, Luk J, Bogdan D, Elmes MW, et al. Fatty-acid-binding protein inhibition produces analgesic effects through peripheral and central mechanisms. *Mol Pain* 2017;13:1744806917697007.
  47. Soukupova M, Palazzo E, De Chiaro M, Gatta L, Migliozi AL, Guida F, et al. Effects of URB597, an inhibitor of fatty acid amide hydrolase (FAAH), on analgesic activity of paracetamol. *Neuro Endocrinol Lett* 2010;31:507-11.
  48. Kwon M, Han J, Kim UJ, Cha M, Um SW, Bai SJ, et al. Inhibition of Mammalian Target of Rapamycin (mTOR) Signaling in the Insular Cortex Alleviates Neuropathic Pain after Peripheral Nerve Injury. *Front Mol Neurosci* 2017;10:79.
  49. Ploghaus A, Tracey I, Gati JS, Clare S, Menon RS, Matthews PM, et al. Dissociating pain from its anticipation in the human brain. *Science* 1999;284:1979-81.
  50. Coffeen U, Canseco-Alba A, Simon-Arceo K, Almanza A, Mercado F, Leon-Olea M, et al. Salvinatorin A reduces neuropathic nociception in the insular cortex of the rat. *Eur J Pain* 2018;22:311-8.
  51. Malek N, Mrugala M, Makuch W, Kolosowska N, Przewlocka B, Binkowski M, et al. A multi-target approach for pain treatment: dual inhibition of fatty acid amide hydrolase and TRPV1 in a rat model of osteoarthritis. *Pain* 2015;156:890-903.
  52. Nasirinezhad F, Jergova S, Pearson JP, Sagen J. Attenuation of persistent pain-related behavior by fatty acid amide hydrolase (FAAH) inhibitors in a rat model of HIV sensory neuropathy. *Neuropharmacology* 2015;95:100-9.
  53. Seillier A, Dominguez Aguilar D, Giuffrida A. The dual FAAH/MAGL inhibitor

- JZL195 has enhanced effects on endocannabinoid transmission and motor behavior in rats as compared to those of the MAGL inhibitor JZL184. *Pharmacol Biochem Behav* 2014;124:153-9.
54. Chae Y, Park HJ, Hahm DH, Lee BH, Park HK, Lee H. Spatiotemporal patterns of neural activity in response to electroacupuncture stimulation in the rodent primary somatosensory cortex. *Neurol Res* 2010;32 Suppl 1:64-8.
  55. Gao YJ, Ji RR. c-Fos and pERK, which is a better marker for neuronal activation and central sensitization after noxious stimulation and tissue injury? *Open Pain J* 2009;2:11-7.
  56. Santos PL, Brito RG, Matos J, Quintans JSS, Quintans-Junior LJ. Fos Protein as a Marker of Neuronal Activity: a Useful Tool in the Study of the Mechanism of Action of Natural Products with Analgesic Activity. *Mol Neurobiol* 2017; doi:10.1007/s12035-017-0658-4.
  57. Starowicz K, Makuch W, Korostynski M, Malek N, Slezak M, Zychowska M, et al. Full inhibition of spinal FAAH leads to TRPV1-mediated analgesic effects in neuropathic rats and possible lipoxygenase-mediated remodeling of anandamide metabolism. *PLoS One* 2013;8:e60040.
  58. Pertwee RG. The diverse CB(1) and CB(2) receptor pharmacology of three plant cannabinoids:  $\Delta(9)$ -tetrahydrocannabinol, cannabidiol and  $\Delta(9)$ -tetrahydrocannabivarin. *British Journal of Pharmacology* 2008;153:199-215.
  59. Zhuo M. Central plasticity in pathological pain. *Novartis Found Symp* 2004;261:132-45; discussion 45-54.
  60. Zhuo M. Contribution of synaptic plasticity in the insular cortex to chronic pain. *Neuroscience* 2016;338:220-9.
  61. Maggio N, Shavit Stein E, Segal M. Cannabidiol Regulates Long Term Potentiation Following Status Epilepticus: Mediation by Calcium Stores and Serotonin. *Front Mol Neurosci* 2018;11:32.
  62. Silva-Cruz A, Carlstrom M, Ribeiro JA, Sebastiao AM. Dual Influence of Endocannabinoids on Long-Term Potentiation of Synaptic Transmission. *Front Pharmacol* 2017;8:921.
  63. Jayamanne A, Greenwood R, Mitchell VA, Aslan S, Piomelli D, Vaughan CW. Actions of the FAAH inhibitor URB597 in neuropathic and inflammatory chronic pain models. *Br J Pharmacol* 2006;147:281-8.
  64. Kinsey SG, Long JZ, O'Neal ST, Abdullah RA, Poklis JL, Boger DL, et al. Blockade of Endocannabinoid-Degrading Enzymes Attenuates Neuropathic Pain. *Journal of Pharmacology and Experimental Therapeutics* 2009;330:902-10.
  65. Centonze D, Bari M, Rossi S, Prosperetti C, Furlan R, Fezza F, et al. The endocannabinoid system is dysregulated in multiple sclerosis and in experimental autoimmune encephalomyelitis. *Brain* 2007;130:2543-53.
  66. Bishay P, Schmidt H, Marian C, Häussler A, Wijnvoord N, Ziebell S, et al. R-Flurbiprofen Reduces Neuropathic Pain in Rodents by Restoring Endogenous Cannabinoids. *PLOS ONE* 2010;5:e10628.
  67. Fegley D, Gaetani S, Duranti A, Tontini A, Mor M, Tarzia G, et al. Characterization of the fatty acid amide hydrolase inhibitor cyclohexyl carbamic acid 3'-carbamoyl-biphenyl-3-yl ester (URB597): effects on anandamide and oleoylethanolamide deactivation. *J Pharmacol Exp Ther* 2005;313:352-8.
  68. Pertwee RG. Ligands that target cannabinoid receptors in the brain: from THC to anandamide and beyond. *Addiction Biology* 2008;13:147-59.

69. Leung D, Saghatelian A, Simon GM, Cravatt BF. Inactivation of N-acyl phosphatidylethanolamine phospholipase D reveals multiple mechanisms for the biosynthesis of endocannabinoids. *Biochemistry* 2006;45:4720-6.
70. Toth A, Boczan J, Kedei N, Lizanecz E, Bagi Z, Papp Z, et al. Expression and distribution of vanilloid receptor 1 (TRPV1) in the adult rat brain. *Brain Res Mol Brain Res* 2005;135:162-8.
71. Kathuria S, Gaetani S, Fegley D, Valino F, Duranti A, Tontini A, et al. Modulation of anxiety through blockade of anandamide hydrolysis. *Nat Med* 2003;9:76-81.

## ABSTRACT (IN KOREAN)

신경 병증성 통증 모델의 뇌섬엽 피질에 작용하는  
FAAH 억제제의 통증 완화 효과

&lt;지도교수 이 배 환&gt;

연세대학교 대학원 의과학과

김민지

뇌섬엽 피질은 통증과 감정의 처리에 관여하는 뇌의 주요한 부위 중 하나이다. 최근 연구에 따르면, IC의 손상은 통증 상실 및 신경 병증성 통증을 완화시키는데 기여하는 것으로 알려져 있다. 내인성 카나비노이드는 통증을 약화시키는 것으로 알려져 있지만, 이 기능을 저해시키는 가수분해 효소 FAAH(fatty acid amide hydrolase)에 의해 내인성 카나비노이드가 생성됨과 동시에 분해된다. FAAH의 활성은 선택적 억제제인 URB597을 통해 억제될 수 있으며, 내인성 카나비노이드의 보존을 통해 통증을 감소효과를 유지시킬 수 있다.

본 연구는 신경 병증성 통증 백서 모델의 뇌섬엽 피질에서 URB597의 진통 효과를 확인하기 위해 수행되었다. 수컷 백서에게 신경 손상을 가하였고 von Frey 검사를 통해 기계적 이질통의 생성을 확인하였다. 신경 병증성 통증군에서 c-Fos, CB1R (cannabinoid receptor 1), NAPE-PLD (N-acyl phosphatidylethanolamine phospholipase D) 및 TRPV1 (transient receptor potential vanilloid 1)의 분자 발현량은 대조군에 비해 유의하게 증가 하였다. 신경 손상 14 일 후 동물모델의 뇌섬엽 피질에 URB597 또는 대조약물을 미세주입 함

으로써 통증완화 효과를 확인하였다. 2 nM 및 4 nM 농도의 URB597을 미세주입한 군에서 기계적 이질통이 유의하게 감소하는 것을 확인하였으며, NAPE-PLD의 발현량 또한 해당 군에서 증가한 것을 확인하였다. 조직학적 분석 및 뇌섬엽 피질의 광영상(optical imaging)을 통해 신경 병증에 의한 신경 활성화 변화 및 URB597 미세주입에 의한 신경 활성화의 감소를 확인하였다.

이러한 결과는 뇌섬엽 피질에서 URB597의 미세주입을 통한 FAAH 억제가 신경 병증으로 인한 뇌섬엽 피질 내의 내인성 카나비노이드 관련 신호의 변화를 조절하고 통증유발과 관련된 신경 흥분성 감소를 유도함으로써 FAAH 신경 병증성 통증을 조절할 수 있는 중요한 기전일 수 있음을 시사한다.

---

핵심되는 말: 뇌섬엽 피질, 신경 병증성 통증, FAAH (Fatty acid amide hydrolase), NAPE-PLD (N-acyl phosphatidylethanolamine phospholipase D), TRPV1 (transient receptor potential vanilloid 1), URB597

## PUBLICATION LIST

**MJ Kim**, BH Lee. A study on the processing and modulation of pain in the insular cortex. *Journal of Applied Subtle Energy*. 2018 Jun 29; Vol. 15, No. 1